International Journal of Fatigue 152 (2021) 106453

Contents lists available at ScienceDirect

International Journal of Fatigue

journal homepage: www.elsevier.com/locate/ijfatigue

Variations on a critical distance theme

A. Navarro *, V. Chaves, J.A. Balbín

Departamento de Ingeniería Mecánica y Fabricación, Escuela Técnica Superior de Ingeniería, Universidad de Sevilla, Camino de los Descubrimientos s/n, 41092 Sevilla, Spain

ARTICLE INFO

Keywords:
Notch
Notched fatigue strength
Notched fatigue limit
Critical distance
Plasticity correction

ABSTRACT

We investigate how the fatigue limit of notched specimens calculated with the Theory of Critical Distance (TCD) changes when variations in the value of the critical distance itself are considered. We motivate our study by showing how attempts at introducing a plastic zone correction in the derivation of the formula for the critical distance lead to a new length which can be significantly larger than the original one. The predictions effected with both lengths were not found to be so different, though. And this led us to study circular holes and V-notches, for which solutions for the ratio K_f/K_t can be derived analytically.

1. Introduction

The method of the critical distance or volume, pioneered by Neuber [1] and Peterson [2], has become a very powerful and reliable tool in the celebrated form proposed by Professor David Taylor [3]. As is well known, this provides, as a first step, a formula to obtain the critical distance for the material in terms of two clearly defined characteristics, namely, the plain fatigue limit of the material and the threshold value of the stress intensity factor. This formula is arrived at when one, basically, applies Peterson's idea to a (long) crack, for which Linear Elastic Fracture Mechanics (LEFM) gives a clear cut propagation criterion. See also the previous work of Tanaka [4].

The second step advocated in the Point Method variant of the critical distance technique is to apply the recommendation of Peterson *literally*, i.e., derive the stress profile in front of the notch and raise the applied load until, at a depth (beyond the notch root) equal to the critical distance, the stress reaches the plain fatigue limit of the material. The notched fatigue limit is the reference applied stress needed to achieve this. Of course, in the majority of cases these calculations are nowadays done using a Finite Element program. Obviously, this was not available to Peterson or Neuber and thus they had to rely on a limited range of notch solutions and different approximations and simplifications to arrive at their respective formulas, which featured characteristic lengths that were typically correlated with the ultimate tensile strength of the material [5–8]. We have described elsewhere [9] how this process of correlation was fraught with difficulties.

The formula furnished by Taylor represents, by comparison, a massive improvement on this account, and it is fair to say that the critical distance method in the definitive formulations of the Point, Line or Area methods has become the tool of choice in practice to calculate the fatigue strength of notched components.

We want to ascertain how sensitive the predicted notched fatigue limit is with respect to possible variations in the critical distance. These variations could arise from errors or uncertainties in the experiments to obtain it, for example. Or it could result from other considerations, as in the present paper. We believe this exploration provides valuable insight into the working of the method itself and gives a good indication of why it works so well in the majority of cases.

2. Nomenclature

K	=	Stress Intensity factor
ΔK	=	Stress Intensity factor range
ΔK_{th}	=	Threshold value of the Stress Intensity factor range
K_f	=	Fatigue notch factor
K_t	=	Elastic stress concentration factor
K_p	=	Effective Stress Intensity factor for the notional crack
L	=	Critical distance
L^*	=	Critical distance with plastic zone correction
r_p	=	Monotonic plastic zone size (estimation)
r_Y	=	Distance from the crack tip where the elastic stress distribution equals the material's yield strength
r^*	=	Distance from the crack tip where the elastic–plastic stress distribution equals the plain fatigue limit of the material

* Corresponding author.
E-mail address: navarro@us.es (A. Navarro).

https://doi.org/10.1016/j.ijfatigue.2021.106453
Received 28 May 2021; Received in revised form 19 July 2021; Accepted 26 July 2021
Available online 30 July 2021

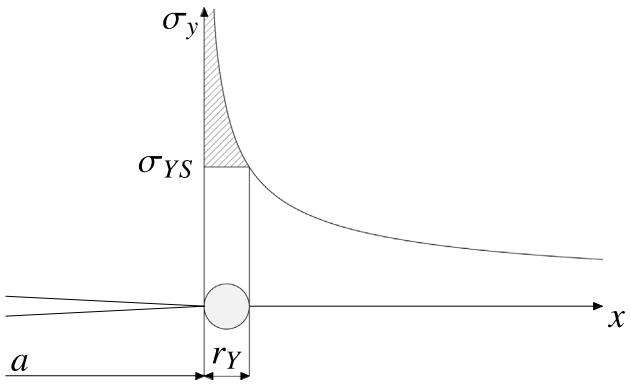

Fig. 1. First estimation of the plastic zone size.

R	=	Stress ratio of the fatigue cycle
Y	=	Geometry correction factor
$\Delta\sigma_{FL}$	=	Plain fatigue limit of the material
$\Delta\sigma_{FL}^{N}$	=	Notched fatigue limit
σ_{YS}	=	Material's yield strength

3. Plastic zone correction to the critical distance

Our point of departure is the realization that, in the derivation of the expression for the critical distance for fatigue through the LEFM threshold condition, it is implicitly assumed that the material behaves in a purely elastic manner. However, most materials deform plastically once the stresses rise to values high enough around the crack tip.

Consider the variation of the stress σ_y in front of the crack tip. It will reach the material's yield strength, σ_{YS}, at some distance from the crack tip, r_Y, and it is assumed that, in the simplest case of an elastic, perfectly plastic material, this is the highest stress the material can sustain. Then it should be clear the force due to the stress shown shaded in Fig. 1 would be lacking in the force balance in the y-direction. Thus the stress curve must be shifted to the right, so that equilibrium is reinstated. As it is well known, this leads to the following reestimation of the (monotonic) plastic zone size

$$r_p = 2r_Y = \frac{1}{\pi}\left(\frac{K}{\sigma_{YS}}\right)^2 \tag{1}$$

For fatigue loading, reverse plastic flow occurs upon reversal of the load in each cycle. This has been analyzed by Rice [10, see his Figure 22]. Suppose loading is reduced by an amount ΔK to a lower level $K - \Delta K$. If crack tip blunting by plastic deformation is neglected, the stress concentration factor is effectively infinite, and reverse plastic flow ensues as soon as the load starts reducing, giving rise to a new zone of reversed plastic deformation inside the plastic zone created by the previous loading. Reloading from $K-\Delta K$ to K restores the situation to the original monotonic plastic zone.

Irwin [12] proposed that the effect of the plastic zone could be accounted for by considering a notional effective crack slightly larger than the actual crack, extending up to the center of the reestimated plastic zone. Thus the crack behaves as if its length were $(a + r_Y)$; see Fig. 2. An effective stress intensity factor, K_p, is obtained by inserting the longer crack length into the K expression for the geometry of interest. Then, the elastic–plastic stress distribution ahead of the plastic zone is (see Saxena [11, p. 16])

$$\sigma_y = \frac{K_p}{\sqrt{2\pi(r - r_Y)}} \tag{2}$$

where

$$K_p = Y(a + r_Y)\,\sigma\sqrt{\pi(a + r_Y)} \tag{3}$$

Since the geometry correction factor, Y, depends on the effective length, which, in turn, depends on the stress intensity factor, an iterative procedure is usually required to solve for K_p; see Anderson [13, p. 64], Kumar [14, p. 107] or Sun and Jin [15, p. 133]. Nevertheless, there are closed-form solutions for some important cases. For example, for the infinite plate with a crack subjected to remote stress σ,

$$K_p = \frac{\sigma\sqrt{\pi a}}{\sqrt{1 - \frac{1}{2}\left(\frac{\sigma}{\sigma_{YS}}\right)^2}} \tag{4}$$

or for the edge crack in a semi-infinite plate

$$K_p = \frac{1.1215\,\sigma\sqrt{\pi a}}{\sqrt{1 - 0.6289\left(\frac{\sigma}{\sigma_{YS}}\right)^2}} \tag{5}$$

It can be seen that the adjusted or effective stress intensity factors reduce to the usual LEFM form when small scale yielding conditions prevail ($\sigma/\sigma_{YS} \ll 1$).

Now, in order to obtain the expression for the critical distance, we write the LEFM condition for crack propagation, namely, that the stress intensity range be equal to the threshold value, and seek the point r^* at which a horizontal line at height equal to the plain fatigue limit of the material, $\Delta\sigma_{FL}$, intersects the stress-distance curve,

$$\Delta\sigma_{FL} = \frac{\Delta K_{th}}{\sqrt{2\pi(r^* - r_Y)}} \tag{6}$$

then

$$r^* = \frac{1}{2\pi}\left(\frac{\Delta K_{th}}{\Delta\sigma_{FL}}\right)^2 + r_Y = \frac{1}{2\pi}\left(\frac{\Delta K_{th}}{\Delta\sigma_{FL}}\right)^2 + \frac{1}{2\pi}\left(\frac{K}{\sigma_{YS}}\right)^2 \tag{7}$$

where K in the last term on the right hand side would be the maximum value of the stress intensity factor in the fatigue cycle. This can also be written in terms of the range and the R-coefficient, $K = \Delta K_{th}/(1 - R)$, so that r^* can be expressed in a more compact fashion

$$r^* = \frac{1}{2\pi}\left(\frac{1}{\Delta\sigma_{FL}^2} + \frac{1}{(1 - R)^2\,\sigma_{YS}^2}\right)\Delta K_{th}^2 \tag{8}$$

In his Point Method (PM), Taylor calls $L/2$ the distance in the stress-distance curve where the stress takes the value of the plain fatigue limit. Then, according to the above calculations, the critical distance with the plastic zone correction, L^*, would be

$$L^* = \frac{1}{\pi}\left(\frac{1}{\Delta\sigma_{FL}^2} + \frac{1}{(1 - R)^2\,\sigma_{YS}^2}\right)\Delta K_{th}^2 \tag{9}$$

Please, bear with us a little more and note that the objective of this paper is not to propose a new formula for the critical distance, but to explore what happens when (not unreasonable, we hope) variations in it are introduced: we have checked this alternative definition in a number of cases, see Tables A.1 and A.2 in the Appendix, expecting that the estimations of the notched fatigue limits effected with it would be really off by a significant amount, given that predictions with the *orthodox* formula are generally so good. But this does not seem to be the case.

Table A.2 shows our calculations and the comparison between the notched fatigue limits obtained for a variety of notches manufactured with the materials given in the previous table. There are some instances where L^* is more than twice L and yet the notched fatigue limits predicted by the Point Method with such different lengths are pretty similar. See for example the results for circular holes in Brass 30/70 reported by Murakami [16]. The average error (in absolute value), with respect to the experimental data, is smaller using the usual formula for the critical distance, 9.70% with L versus 13.49% with L^*. And only in 14 cases out of the 60 analyzed were the predictions with L^* better than those effected with L. But still it seemed to us that, given that on average L^* came out to be 48% bigger than L, the differences

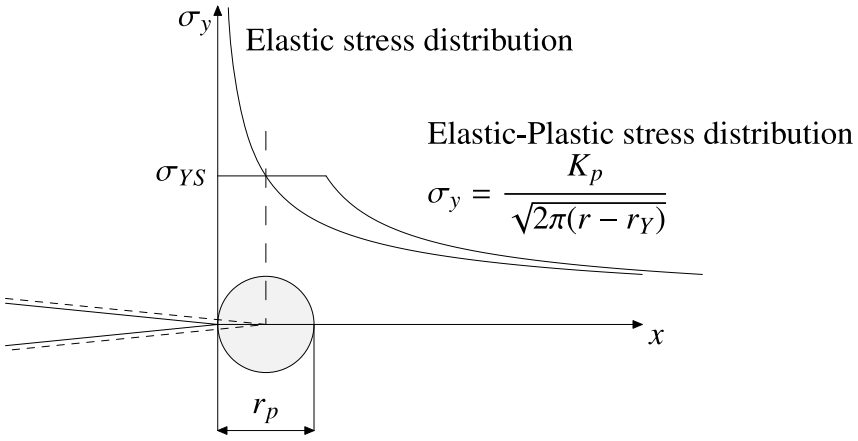

Fig. 2. Notional crack and the elastic–plastic crack tip stress distribution in front of the crack tip (After Saxena [11, Figure 1.9]).

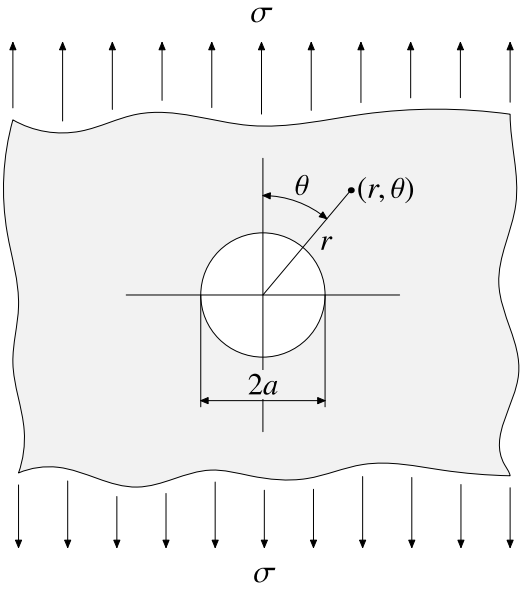

Fig. 3. Circular hole.

in the predicted notched fatigue limits were not all that big (again on average). We found that intriguing, and thus we decided to see if we could check the method at least in some simple cases. It turns out there are analytical solutions that we could use in two important geometries, namely, the circular notch and the rounded V-notch.

4. Circular hole

For the simple case of a circular hole in a thin plate of infinite width under the action of a tensile load (Fig. 3), the stresses at any point (r, θ) from the center of the hole are given by Kirsch's solution [17, p. 91]:

$$\sigma_r = \frac{\sigma}{2}\left(1 - \frac{a^2}{r^2}\right) + \frac{\sigma}{2}\left(1 + \frac{3a^4}{r^4} - \frac{4a^2}{r^2}\right)\cos 2\theta \tag{10}$$

$$\sigma_\theta = \frac{\sigma}{2}\left(1 + \frac{a^2}{r^2}\right) - \frac{\sigma}{2}\left(1 + \frac{3a^4}{r^4}\right)\cos 2\theta \tag{11}$$

$$\tau_{r\theta} = -\frac{\sigma}{2}\left(1 - \frac{3a^4}{r^4} + \frac{2a^2}{r^2}\right)\sin 2\theta \tag{12}$$

The maximum stress occurs at the edge of the hole ($r = a$), in the plane perpendicular to the applied stress ($\theta = \pm\pi/2$) and at this point $\sigma_r = \tau_{r\theta} = 0$, and $\sigma_{\theta,max} = 3\,\sigma$. The distribution of the circumferential stress in this plane is thus

$$\sigma_\theta = \sigma\left(1 + \frac{1}{2}\frac{a^2}{r^2} + \frac{3}{2}\frac{a^4}{r^4}\right) \tag{13}$$

To apply the Point Method one checks the value of the stress at a distance $L/2$ from the notch root. Hence, putting $r = a + L/2$, we have

$$\sigma_\theta = \sigma\left(1 + \frac{1}{2}\frac{a^2}{(a + L/2)^2} + \frac{3}{2}\frac{a^4}{(a + L/2)^4}\right) \tag{14}$$

Now, the critical distance hypothesis says the *notched fatigue limit*, $\Delta\sigma_{FL}^N$, is the *applied cyclic stress range* for which the range of stress at the point at a distance $L/2$ beneath the notch root becomes equal to the *plain fatigue limit* of the material, $\Delta\sigma_{FL}$. Thus, using the previous equation, we can write

$$\Delta\sigma_{FL}^N\left(1 + \frac{1}{2}\frac{a^2}{(a + L/2)^2} + \frac{3}{2}\frac{a^4}{(a + L/2)^4}\right) = \Delta\sigma_{FL} \tag{15}$$

And from here we can calculate the *fatigue notch factor*, K_f, as a function of L and a:

$$K_f = \frac{\Delta\sigma_{FL}}{\Delta\sigma_{FL}^N} = 1 + \frac{1}{2}\frac{a^2}{(a + L/2)^2} + \frac{3}{2}\frac{a^4}{(a + L/2)^4} \tag{16}$$

We normalize with respect to the *stress concentration factor*, $K_t = 3$, to allow further comparisons later

$$\frac{K_f}{K_t} = \frac{1}{3}\left(1 + \frac{1}{2}\frac{a^2}{(a + L/2)^2} + \frac{3}{2}\frac{a^4}{(a + L/2)^4}\right) \tag{17}$$

which can obviously be written in terms of the non dimensional parameter $a/(L/2) = 2a/L$:

$$\frac{K_f}{K_t} = \frac{1}{3}\left(1 + \frac{1}{2}\left(\frac{1}{a/(L/2)} + 1\right)^{-2} + \frac{3}{2}\left(\frac{1}{a/(L/2)} + 1\right)^{-4}\right) \tag{18}$$

Eq. (17) has been plotted in Fig. 4. This graph confirms something that is well known: that when the notch is sufficiently large compared with the "microstructure", little notch sensitivity is observed. In the present context, this means that the notch fatigue limits predicted are very insensitive to the value of L. This is to say, it does not really matter which value we use for L, the notched fatigue strength predicted will vary little, for sufficiently large notches.

However, the graph also shows that for very small holes there will be a more strong influence of the particular value of L chosen for the calculation. See, for example, the line corresponding to $a = 0.1$ mm, which marks the upper frontier of the darkest blue region, at the left lower side of the figure. Notice its pronounced gradient in the region where L is very small. This steepness, however, can be a bit misleading, and a better idea of how big this influence is can be gained as follows. Given the values of the ratios between L^* and L shown in Table A.1, we decided to see what would happen if the value of the critical distance

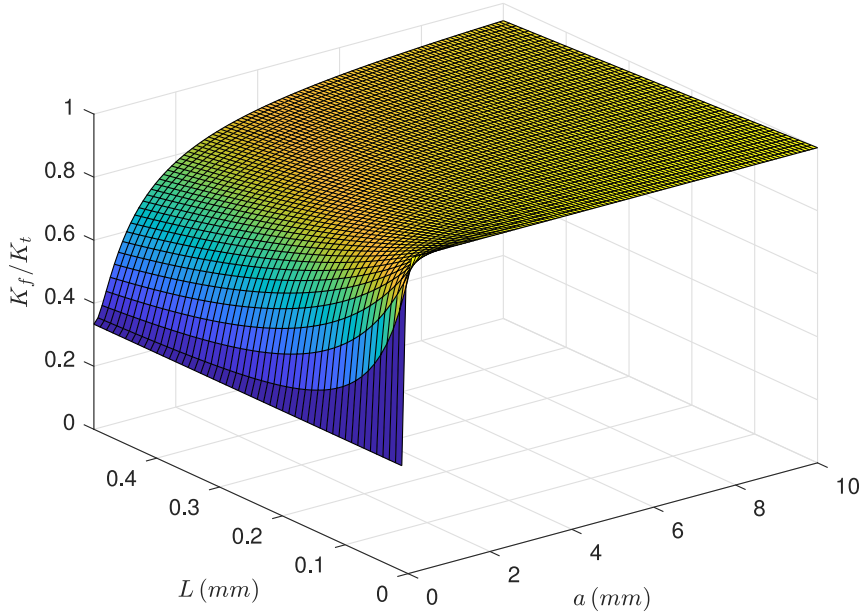

Fig. 4. K_f/K_t for the circular hole as a function of L and a.

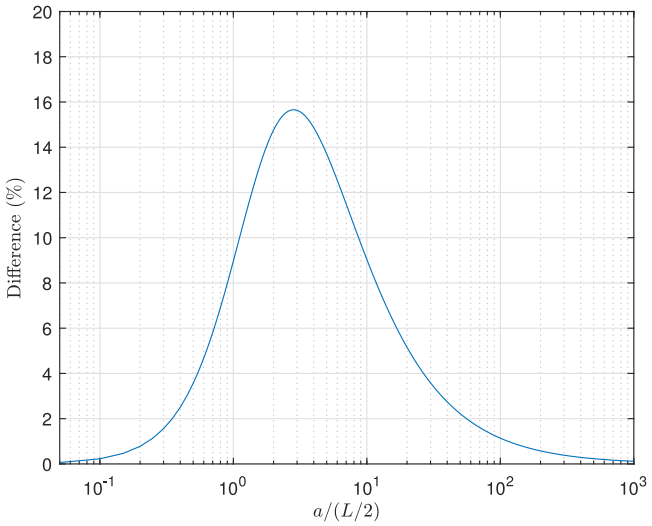

Fig. 5. Difference in K_f/K_t when calculated using $1.5\,L$ instead of L.

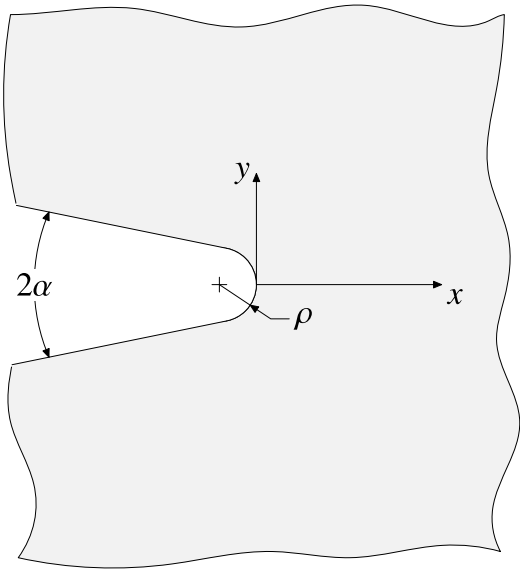

Fig. 6. V-notch.

used in the Point Method were to be increased (or reduced) by as much as one half. This is most easily done here. Since K_f/K_t depends really only on the parameter $2a/L$, for any value of this parameter we can calculate K_f/K_t and compare it with the value that we would obtain using $2a/1.5/L$ instead. This is shown in Fig. 5. It can be seen that the biggest difference is about 15.6%, when the hole diameter is about 3 times L. We just notice that this is within the error interval of about 20% usually quoted when assessing the accuracy of the critical distance techniques.

5. V-notch

Several researchers [18–20] have pointed out that, in the vicinity of a V-notch tip, stress distributions are very similar: there are "universal features". The stress concentration factor K_t introduces the information about the remote applied loads and the overall geometry in the stress solution near the notch root, much in the same way that the stress intensity factor introduces the information about the crack size, component geometry and applied stresses into the universal crack tip stress field (the so-called K-field).

Filippi, Lazzarin and Tovo [21] have given explicit formulas for calculating the circumferential stress along the bisector of notches having opening angles 2α (see Fig. 6) equal to 0, 45, 90 and 135 degrees:

$$2\alpha = 0^\circ \qquad \frac{\sigma_{max}}{2\sqrt{2}}\,\rho^{0.5}\left[(x+0.5\rho)^{-0.5}+0.5\rho(x+0.5\rho)^{-1.5}\right] \tag{19}$$

$$2\alpha = 45^\circ \qquad \frac{\sigma_{max}}{3.221}\,\rho^{0.4950}\left[1.0514(x+0.4286\rho)^{-0.4950} + 0.4820\rho^{0.9369}\,(x+0.4286\rho)^{-1.4319}\right] \tag{20}$$

$$2\alpha = 90^\circ \qquad \frac{\sigma_{max}}{3.874}\,\rho^{0.4555}\left[1.2976(x+0.3333\rho)^{-0.4555} + 0.3957\rho^{0.8894}\,(x+0.3333\rho)^{-1.3449}\right] \tag{21}$$

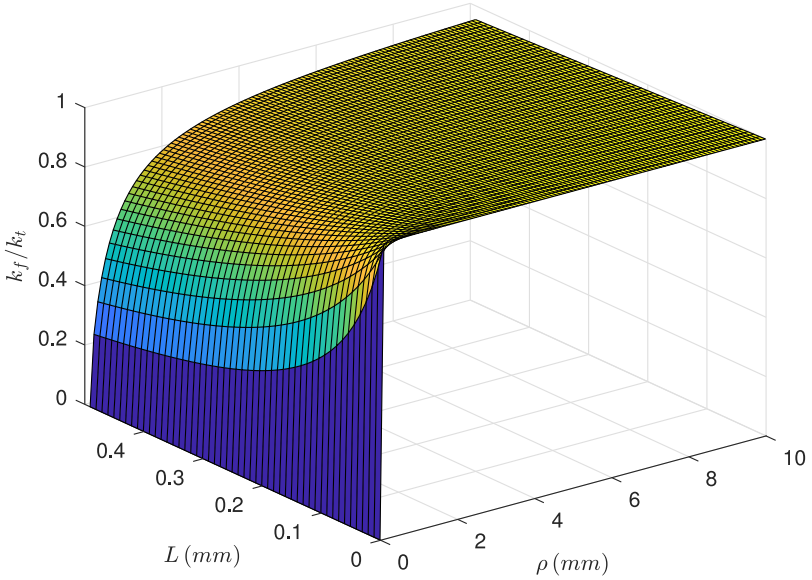

Fig. 7. K_f/K_t for the V-Notch as a function of L and ρ ($2\alpha = 0$).

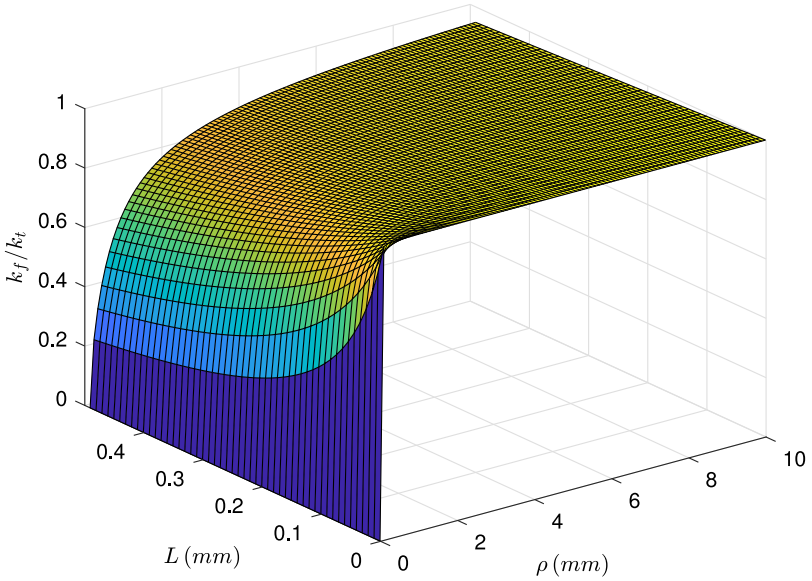

Fig. 8. K_f/K_t for the V-Notch as a function of L and ρ ($2\alpha = 45°$).

$$2\alpha = 135° \qquad \frac{\sigma_{max}}{4.940}\ \rho^{0.3264}\left[2.040(x+0.2\rho)^{-0.3264} + 0.2091\rho^{0.8934}\,(x+0.2\rho)^{-1.2198}\right] \tag{22}$$

Although these equations are strictly only valid for infinite notched plates, the results have been shown to be quite accurate for finite specimens, at least up to the point where the stress becomes equal to the net stress on the minimum cross section of symmetrical doubled-notched specimens.

It is convenient to write formally the equations above as

$$\sigma_\theta = \sigma_{max}\ f_\alpha(x,\rho) = K_t\,\sigma_{nom}\ f_\alpha(x,\rho) \tag{23}$$

where σ_{max} has also been expressed as the product of the stress concentration factor K_t and the applied nominal stress σ_{nom}. Now, as claimed before, the notched fatigue limit $\Delta\sigma_{FL}^N$ is the value of applied nominal stress which makes the stress at the distance $L/2$ equal to the plain fatigue limit of the material, $\Delta\sigma_{FL}$, according to the Point Method. We thus write

$$\Delta\sigma_\theta\,(x = L/2) = \Delta\sigma_{FL} = K_t\ \Delta\sigma_{FL}^N\ f_\alpha(L/2,\rho) \tag{24}$$

Then we see that

$$\frac{K_f}{K_t} = f_\alpha(L/2,\rho) \tag{25}$$

This can be plotted for the four angles for which the functions $f_\alpha(L/2,\rho)$ can be obtained from Eqs. (19) to (22) above. Notice that, again, they can be written in a more revealing form as functions of the single non dimensional parameter $\rho/(L/2) = 2\rho/L$. For example, for $2\alpha = 45°$, we would have

$$f_{45°} = \frac{\sigma_{max}}{3.221}\left[1.0514\left(\frac{1}{\rho/(L/2)} + 0.4286\right)^{-0.4950} + 0.4820\left(\frac{1}{\rho/(L/2)} + 0.4286\right)^{-1.4319}\right] \tag{26}$$

Figs. 7 to 10 show K_f/K_t as a function of L and ρ for the four angles chosen. Let us recall that K_t does not depend on L. It just depends on ρ (and the notch angle, of course). We can see that, roughly, the comments made for the circular hole are applicable here too. There is

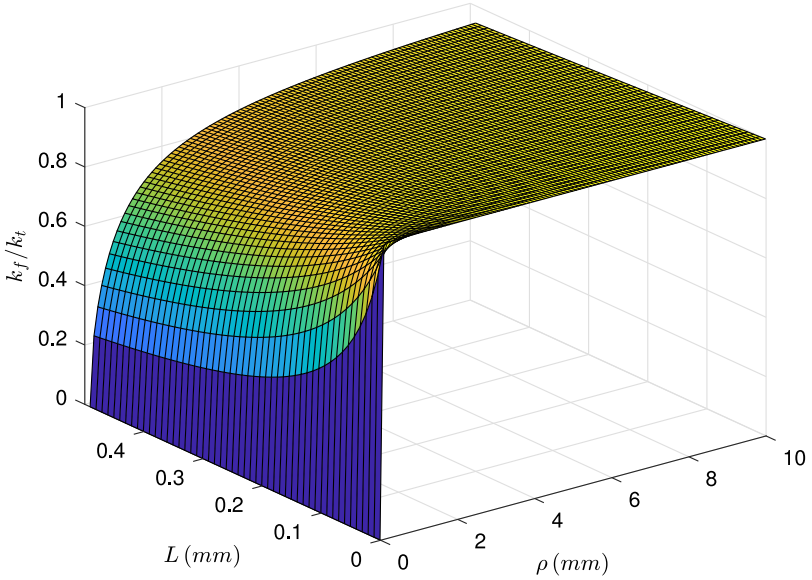

Fig. 9. K_f/K_t for the V-Notch as a function of L and ρ ($2\alpha = 90°$).

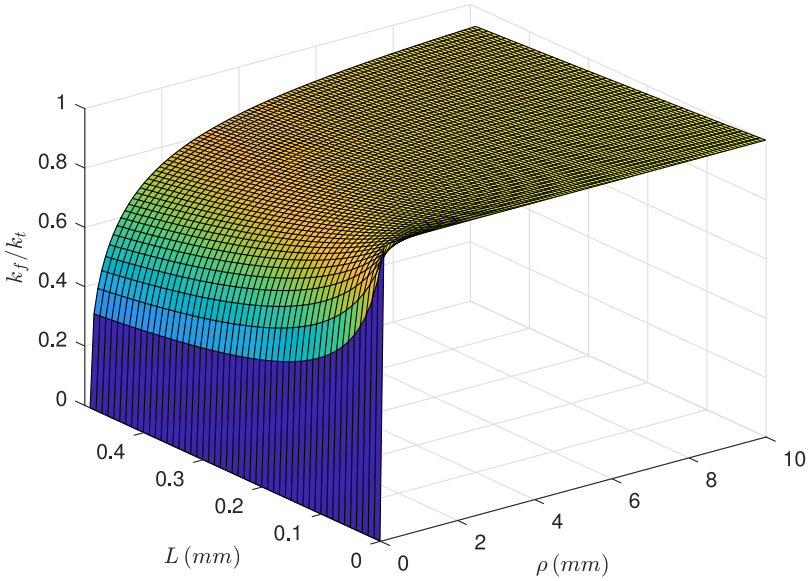

Fig. 10. K_f/K_t for the V-Notch as a function of L and ρ ($2\alpha = 135°$).

a plateau, an extended tableland where K_t/K_f varies very smoothly with L for any value of ρ. But there is also a pronounced fall at the left edge of the plateau. The "blue wall" of the figures corresponds to the situation where the root radius is very small and there is almost a singularity in the stress field. Fatigue propagation is therefore tightly controlled by the threshold condition. Thus errors in L should be less forgiving.

Again, we check what happens if the value of the critical distance used in the Point Method were increased (or reduced) by as much as one half. And, as before, since K_f/K_t depends solely on $2\rho/L$, as per Eq. (26) for $2\alpha = 45°$, and likewise for the other angles, we calculate K_f/K_t for every value of $2\rho/L$ and then recalculate again K_f/K_t but this second time using $1.5L/2$, i.e., $2\rho/1.5/L$ for the non dimensional parameter. We then compare it with the value that we obtained in the first place.

The results are shown in Figs. 11 to 14. Now, of course, for the sharpest angles of 0°, the difference between the two calculations tends to 22.48%, corresponding to $(\sqrt{1.5} - 1)$, when ρ tends to zero, as expected. And the "error" peaks at 24.25% for $2\rho/L = 0.46$. The results are pretty similar for 45°. The differences diminish as the angle of the notch becomes wider. For the case 135°, they are everywhere below 15%. We notice that, for the four notch angles studied, when the tip radii becomes larger than L (i.e. $2\rho/L \geq 2$), the difference between making the calculations with L or $1.5L$ becomes smaller than 20%. Just to put this in context, note that the average value of L for 67 steels reported by Susmel in Appendix A of his book [22] is 0.141 mm, the maximum and minimum being 0.782 and 0.005 mm, respectively.

It has not escaped our notice that the specific pairing we have postulated in defining the non-dimensional variable above, namely $\rho/(L/2)$, implies that the same differences could also arise from changes in the notch tip radius, ρ, rather than in L. This would provide some additional rationale for using two common simplifications in the FEA analysis of components in the context of TCD, namely, the use of relatively coarse meshes and defeaturing (see [23–25]). We are referring to the fact that typical element sizes used in industry for routine analyses by Finite Elements need not be too dense. Also, to the use of models

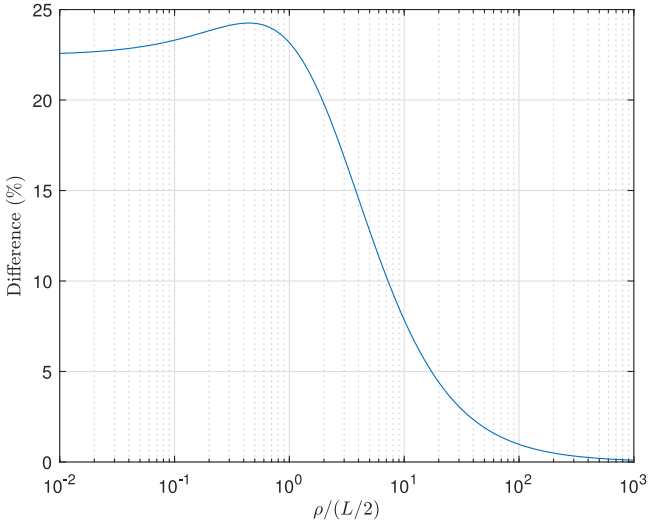

Fig. 11. Difference in K_f/K_t when calculated using $1.5\,L$ instead of L. V-notch with $2\alpha = 0°$.

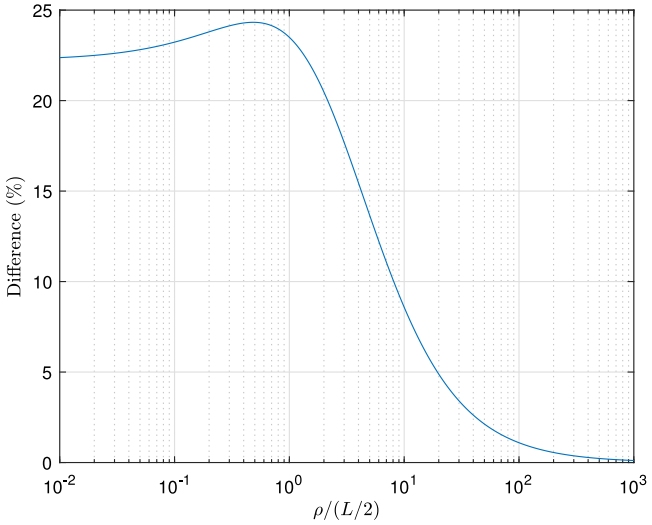

Fig. 12. Difference in K_f/K_t when calculated using $1.5\,L$ instead of L. V-notch with $2\alpha = 45°$.

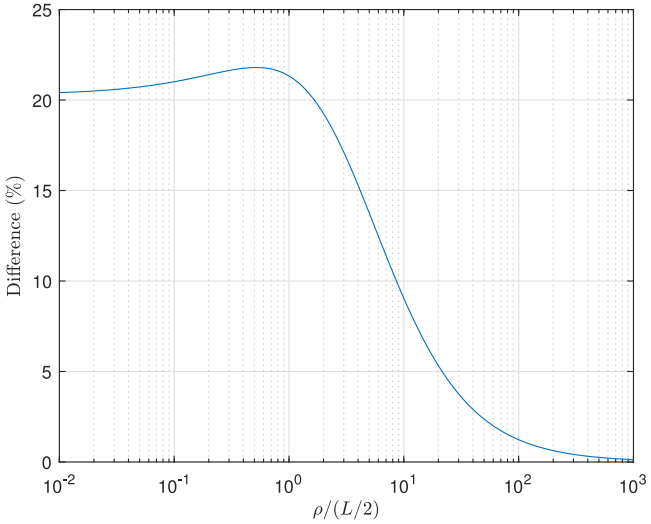

Fig. 13. Difference in K_f/K_t when calculated using $1.5\,L$ instead of L. V-notch with $2\alpha = 90°$.

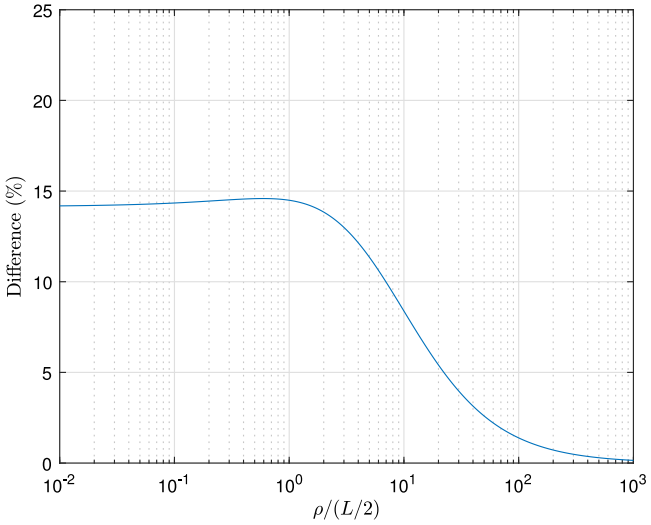

Fig. 14. Difference in K_f/K_t when calculated using $1.5\,L$ instead of L. V-notch with $2\alpha = 135°$.

where some features of the real component are missing or simplified, such as, for example, employing a model where a corner with a finite root radius is represented without the radius.

6. Conclusions

- We have analyzed the sensitivity of fatigue limits of notched specimens calculated with the Theory of Critical Distance with respect to variations in the value of the critical distance itself.
- Introducing a plastic zone correction in the derivation of the formula for the critical distance leads to a new length which can be significantly larger than the original one.
- However, it is found that such differences in the value of the critical distance do not carry over into the computed value of the notched fatigue limits.
- For a wide range of notches, the value of the critical distance used for calculating the notched fatigue strength does not actually seem to be so critical.
- This has been established by looking at circular holes and V-notches, for which solutions for the ratio K_f/K_t can be derived analytically.
- It would appear that building graphs such as those depicting the sort of tableland distribution for K_f/K_t shown above could be useful in fatigue analyses of practical components.

Acknowledgments

The authors would like to thank the European Union, the Spanish Government and the Junta de Andalucía, Spain for its financial support through grants DPI2017-84788-P (FEDER/Ministerio de Ciencia e Innovación - Agencia Estatal de Investigación) and P18-FR-4306 ("Fondo Europeo de Desarrollo Regional (FEDER) y Consejería de Economía, Conocimiento, Empresas y Universidad de la Junta de Andalucía, dentro del Programa Operativo FEDER 2014–2020").

Appendix. Tables

See Tables A.1 and A.2.

Table A.1
Materials and geometries of notched components from the literature.

Material	$\Delta\sigma_{FL}$ (MPa)	σ_{YS} (MPa)	ΔK_{th} (MPa)	L (mm)	L^* (mm)	Geometry[a]	Loading	R	Reference
0.46% C steel annealed	480	284	10.42	0.150[b]	0.257	CHB	Rot. Bending	−1	Murakami [26]
0.13% C steel	362	206	11.00	0.294[c]	0.521	CHB	Rot. Bending	−1	Murakami [26]
Al alloy 2017-T4	313.8[d]	368.7	11.51	0.428[i]	0.506	CHB	Rot. Bending	−1	Murakami [16]
Brass 70/30	245.2[d]	103	6.39	0.216[i]	0.522	CHB	Rot. Bending	−1	Murakami [16]
0.37% C steel	470	328[e]	15.36	0.340[f]	0.515	CHB	Rot. Bend., Axial	−1	Endo [27]
1045 steel	606	466	13.84	0.166	0.236	CHP	Axial	−1	DuQuesnay et al. [28]
Al alloy 2024-T351	248[g]	360	7.09	0.260	0.291	CHP	Axial	−1	DuQuesnay et al. [28]
Al 7075	516[h]	595	7.76	0.072[i]	0.086	CHB	Axial	−1	Chaves et al. [29]
Stainless steel	632	467	15.03	0.180[j]	0.262	CHB	Axial	−1	Chaves et al. [30]
Mild steel	400	293.4[k]	12.88	0.330	0.483	ENP	Axial	−1	Frost et al. [31,32]
Mild steel(2)	446	339.7[l]	12.99	0.270	0.386	CNB	Axial	−1	Frost et al. [31,32]
Al alloy B.S. L 65	300[m]	432.3[l]	4.19	0.062[c]	0.070	CNB	Axial	−1	Frost [33]
SM41B steel	326	194	12.36	0.458	0.781	CNP	Axial	−1	Tanaka et al. [34]
15313 steel	440	380	12.01	0.237	0.316	CNB	Axial	−1	Lukas et al. [35]
Al alloy AA356	231[n]	192	3.95	0.093	0.127	CNB	Rot. Bending	−1	Atzori et al. [36]

[a]CHB = center hole in cylindrical bar, CHP = center hole in plate, ENP = edge notched plate, CNB = circumferential notch in cylindrical bar, CNP = center notch in plate.
[b][3].
[c][22].
[d]Fatigue endurance at $3 \cdot 10^7$ cycles.
[e][37].
[f][38].
[g]Fatigue endurance at 10^7 cycles.
[h]Fatigue endurance at 10^6 cycles.
[i]Estimated as $L = 3.1^2 D/2$ (see [9]).
[j][39].
[k][40].
[l][33].
[m]Fatigue endurance at $50 \cdot 10^6$ cycles.
[n]Fatigue endurance at $2 \cdot 10^6$ cycles.

Table A.2
Comparison of notched fatigue limits predicted with L and L^*.

Material	Ref.	Notch		Notched fatigue limit					Remarks
		Depth	Radius	Experimental	Point Method (L)		Point Method (L^*)		
		(mm)	(mm)	$\Delta\sigma_{FL}^N$ (MPa)	$\Delta\sigma_{FL}^N$ (MPa)	Error (%)[a]	$\Delta\sigma_{FL}^N$ (MPa)	Error (%)[a]	
0.46%C steel	[26]	0.02	0.02	470.0	468.2	−0.4	475.5	1.2	
		0.025	0.025	452.0	462.8	2.4	473.2	4.7	
		0.04	0.04	422.0	443.4	5.1	464.7	10.1	
		0.05	0.05	402.0	429.2	6.8	457.8	13.9	
		0.1	0.1	362.0	362.8	0.2	417.1	15.2	
		0.25	0.25	314.0	263.6	−16.1	319.3	1.7	
0.13%C steel	[26]	0.04	0.04	344.0	352.8	2.6	358.7	4.3	
		0.05	0.05	344.0	348.6	1.3	357.0	3.8	
		0.1	0.1	294.0	322.6	9.7	345.6	17.6	
		0.25	0.25	256.0	252.4	−1.4	300.1	17.2	
Al 2017-T4	[16]	0.05	0.05	294.2	307.7	4.6	309.2	5.1	
		0.1	0.1	245.2	294.3	20.0	298.9	21.9	
Brass 70/30	[16]	0.05	0.05	235.4	230.2	−2.2	241.8	2.7	
		0.1	0.1	215.8	205.1	−5.0	234.1	8.5	
		0.25	0.25	196.2	153.2	−21.9	203.4	3.7	
0.37%C steel	[27]	0.05	0.05	390.0	456.4	17.0	463.4	18.8	
		0.25	0.25	300.0	344.2	14.7	388.4	29.5	
1045 steel	[28]	0.12	0.12	360.0	446.3	24.0	495.2	37.5	
		0.25	0.25	310.0	344.6	11.2	391.0	26.1	
		0.5	0.5	276.0	278.1	0.8	307.7	11.5	
		1.5	1.5	248.0	228.0	−8.1	238.8	−3.7	
Al 2024-T351	[28]	0.12	0.12	160.0	207.6	29.7	212.9	33.1	
		0.25	0.25	124.0	165.6	33.6	172.3	38.9	
		0.5	0.5	124.0	129.8	4.7	134.8	8.7	
		1.5	1.5	90.0	99.2	10.3	101.2	12.4	
Al 7075	[29]	0.5	0.5	190.0	200.7	5.6	206.0	8.4	
		1.00	1.00	188.0	186.4	−0.8	189.1	0.6	
		1.5	1.5	170.0	181.6	6.8	183.4	7.9	
Stainless steel	[30]	0.5	0.5	320.0	296.3	−7.4	331.9	3.7	
		1.00	1.00	308.0	254.5	−17.4	274.0	−11.0	
		1.5	1.5	282.0	240.0	−14.9	253.3	−10.2	

(*continued on next page*)

Table A.2 (*continued*).

Material	Ref.	Notch		Notched fatigue limit					Remarks
		Depth	Radius	Experimental	Point Method (L)		Point Method (L^*)		
		(mm)	(mm)	$\Delta\sigma_{FL}^{N}$ (MPa)	$\Delta\sigma_{FL}^{N}$ (MPa)	Error (%)[a]	$\Delta\sigma_{FL}^{N}$ (MPa)	Error (%)[a]	
Mild steel	[31]	5.08	0.102	100.4	99.5	−0.9	122.0	21.6	[b] K_{tn} = 14.3, V-angle=55°
		5.08	0.254	108.0	95.6	−11.5	116.1	7.5	K_{tn} = 9.2, V-angle=55°
		5.08	0.508	100.4	98.1	−2.3	114.6	14.1	K_{tn} = 6.7, V-angle=55°
		5.08	1.27	123.6	114.2	−7.6	124.9	1.0	K_{tn} = 4.5, V-angle=55°
		5.08	7.62	185.2	189.4	2.3	193.6	4.5	K_{tn} = 2.2, V-angle=55°
Mild steel (2)	[31]	5.08	0.05	115.8	128.4	10.9	152.9	32.0	K_{tn} = 13.8, V-angle=55°
		5.08	0.1	108.0	123.5	14.3	149.3	38.2	K_{tn} = 11.2, V-angle=55°
		5.08	0.254	115.8	119.3	3.0	141.3	22.0	K_{tn} = 7.5, V-angle=55°
		5.08	0.508	115.8	125.4	8.2	142.9	23.4	K_{tn} = 5.4, V-angle=55°
		5.08	1.27	131.2	150.4	14.7	161.9	23.4	K_{tn} = 3.6, V-angle=55°
Al alloy B.S. L 65	[33]	5.08	0.1	46.4	41.2	−11.3	42.8	−7.7	K_{tn} = 11.2, V-angle=55°
		5.08	0.2	46.4	46.7	0.7	48.0	3.5	K_{tn} = 8.3, V-angle=55°
		5.08	0.508	61.8	61.8	0.1	62.6	1.4	K_{tn} = 5.4, V-angle=55°
		5.08	1.27	92.6	87.2	−5.8	87.7	−5.3	K_{tn} = 3.6, V-angle=55°
SM41B steel	[34]	3.00	0.16	120.0	109.8	−8.5	143.8	19.8	K_{tn} = 9.9, Elliptical
		3.00	0.39	120.0	105.5	−12.1	137.6	14.6	K_{tn} = 6.7, Elliptical
		3.00	0.83	110.0	108.6	−1.3	134.4	22.2	K_{tn} = 4.8, Elliptical
		3.00	3.00	150.0	143.1	−4.6	158.0	5.4	K_{tn} = 2.7
15313 steel	[35]	0.015	0.015	440.0	443.8	0.9	444.6	1.0	
		0.03	0.03	440.0	442.3	0.5	446.5	1.5	
		0.05	0.05	420.0	434.7	3.5	444.8	5.9	
		0.07	0.07	330.0	420.6	27.5	438.1	32.8	
		0.2	0.2	280.0	341.2	21.8	378.0	35.0	
		0.4	0.4	300.0	301.9	0.6	334.3	11.4	
		0.75	0.75	320.0	310.3	−3.0	333.8	4.3	
Al AA356	[36]	0.24	0.1	114.8	102.3	−10.9	118.3	3.0	K_{tg} = 4.3, V-angle=79.9°
		0.63	0.18	109.8	65.5	−40.4	73.6	−33.0	K_{tg} = 5.4, V-angle=59.2°
		1.3	0.09	44.8	34.9	−22.1	40.7	−9.1	K_{tg} = 13.1, V-angle=60.3°
		2.9	0.08	17.7	13.4	−24.5	15.7	−11.3	K_{tg} = 36.4, V-angle=68.3°

[a]Error = (Predicted-Experimental)/Experimental×100.

[b]K_{tn}, stress concentration factor referred to net area. K_{tg} referred to gross area.

References

[1] Neuber H. Kerbspannungslehre Theorie Der Spannungskonzentration Genaue Berechnung Der Festigkeit. 4. auflage. Springer-Verlag; 2001, There is an English translation of an ealier edition, Theory of notch stresses: principles for exact calculation of strength with reference to structural form and material. Edwards JW. Ann Arbor, MI; 1946.

[2] Peterson RE. Notch sensitivity. In: G. Sines, J.L. Waisman, editors. Metal fatigue. McGraw-Hill; 1959, p. 293–306.

[3] Taylor D. The theory of critical distances: A new perspective in fracture mechanics. Elsevier Science; 2010.

[4] Tanaka K. Engineering formulae for fatigue strength reduction due to crack-like notches. Int J Fract 1983;22(2):R39–46.

[5] Langer BF. Application of stress concentration factors. In: Bettis technical review. Reactor technology. WAPD-BT-18. Pittsburgh: Westinghouse Electric Corp. Bettis Atomic Power Lab.; 1960.

[6] Kuhn P, Hardrath HF. An engineering method for estimating notch-size effect in fatigue tests on steel. NACA technical note 2805, NACA; 1952.

[7] Mitchell MR. Fundamentals of modern fatigue analysis for design. In: Lampman SR, editor. ASM Handbook Volume 19: Fatigue and Fracture. Material Park, OH: ASM International.; 1996, p. 227–49.

[8] Rice RC, editor. SAE Fatigue Design Handbook. Warrendale, PA: Society of Automotive Engineers; 1997.

[9] Navarro A, Vallellano C, de los Rios ER, Xin XJ. Notch sensitivity and size effects described by a short crack propagation model. In: Beynon JH, Brown MW, Smith RA, Lindley TC, Tomkins B, editors. Engineering Against Fatigue. Balkema Publishers; 1997, p. 63–72.

[10] Rice JR. Mechanics of crack tip deformation and extension by fatigue. In: Grosskreutz J, editor. Fatigue Crack Propagation, ASTM STP 415. West Conshohocken, PA: ASTM International; 1967, p. 247–311.

[11] Saxena A. Advanced fracture mechanics and structural integrity. CRC Press; 2019.

[12] Irwin G. Plastic zone near a crack and fracture toughness. In: Mechanical and Metallurgical Behavior of Sheet Materials, Proceedings of the Seventh Sagamore Ordnance Materials Research Conference. Sagamore Conference Center Racquette Lake; 1960, p. VI–63–VI–78.

[13] Anderson T. Fracture mechanics: fundamentals and applications. Fourth ed.. CRC Press; 2017.

[14] Kumar P. Elements of fracture mechanics. Tata McGraw-Hill Publishing Company Limited; 2009.

[15] Sun C, Jin Z. Fracture mechanics. Elsevier Science; 2011.

[16] Murakami Y, Tazunoki Y, T. Endo. Existence of the coaxing effect and effects of small artificial holes on fatigue strength of an aluminum alloy and 70-30 brass. Metall Trans A 1984;15(11):2029–38.

[17] Timoshenko S, Goodier J. Theory of elasticity (international student edition). Third ed.. McGraw-Hill; 1982.

[18] Schijve J. Stress gradients around notches. Fatigue Fract Eng Mater Struct 1980;3(4):325–38.

[19] Glinka G, Newport A. Universal features of elastic notch-tip stress fields. Int J Fatigue 1987;9(3):143–50.

[20] Lazzarin P, Tovo R. A unified approach to the evaluation of linear elastic stress fields in the neighborhood of cracks and notches. Int J Fract 1996;78(1):3–19.

[21] Filippi S, Lazzarin P, Tovo R. Developments of some explicit formulas useful to describe elastic stress fields ahead of notches in plates. Int J Solids Struct 2002;39(17):4543–65.

[22] Susmel L. Multiaxial notch fatigue. Woodhead Publishing; 2009.

[23] Chaves V. Use of simplified models in fatigue prediction of components with stress concentrations [Master's thesis], Trinity College Dublin; 2002.

[24] Chaves V, Taylor D. Use of simplified models in fatigue prediction of engineering components. In: Proceedings of the 8th international fatigue conference, vol. 5. 2002, p. 2799–806.

[25] Meneghetti G, Campagnolo A, Berto F. Assessment of tensile fatigue limit of notches using sharp and coarse linear elastic finite element models. Theor Appl Fract Mech 2016;84:106–18.

[26] Murakami Y. Metal fatigue: effects of small defects and nonmetallic inclusions. Elsevier Science; 2019.

[27] Endo M. Effects of small defects on the fatigue strengths of steel and ductile iron under combined axial/torsional loading. In: Ravichandran KS, Ritchie ROMY, editors. Small fatigue cracks: mechanics mechanisms and applications. Elsevier; 1999, p. 375–87.

[28] DuQuesnay DL, Topper TH, Yu MT. The effect of notch radius on the fatigue notch factor and the propagation of short cracks. In: Miller KJ, de los Rios ER, editors. The behaviour of short fatigue cracks. London: EGF Pub. 1. Mechanical Engineering Publication; 1986, p. 323–35.

[29] Chaves V, Beretta G, Balbín J, Navarro A. Fatigue life and crack growth direction in 7075-t6 aluminium alloy specimens with a circular hole under biaxial loading. Int J Fatigue 2019;125:222–36.

[30] Chaves V, Navarro A, Madrigal C. Stage I crack directions under in-phase axial-torsion fatigue loading for AISI 304L stainless steel. Int J Fatigue 2015;80:10–21.

[31] Frost NE. A relation between the critical alternating propagation stress and crack length for mild steel. Proc Instn Mech Engrs 1959;173:811–27.
[32] Frost NE, Pook L, Denton K. A fracture mechanics analysis of fatigue crack growth data for various materials. Eng Fract Mech 1971;3(2):109–26.
[33] Frost NE. Non-propagating cracks in vee-notched specimens subject to fatigue loading. Aeronaut Q 1957;8(1):1–20.
[34] Tanaka K, Akiniwa Y. Resistance-curve method for predicting propagation threshold of short fatigue cracks at notches. Eng Fract Mech 1988;30(6):863–76.
[35] Lukas P, Kunz L, Weiss B, Stickler R. Non-damaging notches in fatigue. Fatigue Fract Eng Mater Struct 1986;9(3):195–204.
[36] Atzori B, Meneghetti G, Susmel L. Fatigue behaviour of AA356-T6 cast aluminium alloy weakened by cracks and notches. Eng Fract Mech 2004;71(4):759–68.
[37] Endo M, Ishimoto I. The fatigue strength of steels containing small holes under out-of-phase combined loading. Int J Fatigue 2006;28(5):592–7.
[38] Carpinteri A, Spagnoli A, Vantadori S, Viappiani D. A multiaxial criterion for notch high-cycle fatigue using a critical-point method. Eng Fract Mech 2008;75(7):1864–74.
[39] Beretta G. Fatiga en componentes con concentradores de Tensión Bajo Carga Biaxial [Ph.D. thesis], Universidad de Sevilla; 2016.
[40] Frost NE, Dugdale DS. Fatigue tests on notched mild steel plates with measurements of fatigue cracks. J Mech Phys Solids 1957;5(3):182–92.